Fluid Phase Equilibria 268 (2008) 74–84

Contents lists available at ScienceDirect

Fluid Phase Equilibria

journal homepage: www.elsevier.com/locate/fluid

Evaluation of COSMO-RS for the prediction of LLE and VLE of water and ionic liquids binary systems

Mara G. Freire[a], Sónia P.M. Ventura[a], Luís M.N.B.F. Santos[b], Isabel M. Marrucho[a], João A.P. Coutinho[a,*]

[a] CICECO, Departamento de Química, Universidade de Aveiro, 3810-193 Aveiro, Portugal
[b] CIQ, Departamento de Química, Faculdade de Ciências da Universidade do Porto, R. Campo Alegre 687, 4169-007 Porto, Portugal

ARTICLE INFO

Article history:
Received 13 February 2008
Received in revised form 11 April 2008
Accepted 14 April 2008
Available online 22 April 2008

Keywords:
Ionic liquids
Water
LLE
VLE
COSMO-RS

ABSTRACT

Ionic liquids (ILs) have achieved special and dedicated attention from the scientific community in recent years and a large number of studies involving different features of properties and applications of ILs have been presented. The complete understanding of the phase behaviour of ILs with water is an important issue yet there are few experimental data on their phase equilibria. In this work the predictive capability of COSMO-RS, a predictive model based on unimolecular quantum chemistry calculations, was evaluated for the description of the liquid–liquid equilibria (LLE) and the vapour–liquid equilibria (VLE) of diverse binary mixtures of water and ILs. The effect of the ions conformers on the quality of the predictions was assessed and the quantum chemical COSMO calculation at the BP/TZVP level derived from the lowest energy conformations was adopted. While the LLE predictions degrade with increasing the hydrophilic IL anion character, in general a good qualitative agreement between the model predictions and experimental VLE and LLE data was obtained. COSMO-RS showed to be very helpful as an *a priori* predictive method in order to find suitable candidates for a certain task or specific applications before extensive experimental measurements.

1. Introduction

Room-temperature ionic liquids (ILs) are salts commonly composed of relatively large organic cations and inorganic or organic anions that remain liquid at or near room temperature. Unlike molecular liquids, the ionic nature of these liquids results in a unique combination of intrinsic physical and chemical properties for most of them, such as high thermal stability, large liquidus range, high ionic conductivity, negligible vapour pressure, non-flammability and a highly solvating capacity for a wide range of organic, inorganic and organometallic compounds.

Among the several applications foreseeable for ILs in the chemical industry there has been considerable interest in the potential of ILs for separation processes as extraction media where, among others, ILs have shown promising in the liquid–liquid extraction of organics from water [1–3]. For the extraction of organic products from chemical reactions that proceed in aqueous media and for liquid–liquid extractions from aqueous phases, ILs with lower solubility in water are required. While they cannot contribute to air pollution due to their negligible vapour pressures, they do have in fact a significant solubility in water and, as a result, this is the most likely medium through which ILs will enter the environment. Moreover, the loss of ILs into the aqueous phase may be an important factor in estimating the cost of the IL recycling steps and the cost of water treatments. Furthermore, there was found a relation between the ILs hydrophobicity nature and their aquatic toxicity level [4,5], and the knowledge of the liquid phase behaviour between water and ILs can be a way to assess and predict the ILs environmental impact.

Abbreviations: [C_2mim][Tf_2N], 1-ethyl-3-methylimidazolium bis(trifluoromethylsulfonyl)imide; [C_3mim][Tf_2N], 1-methyl-3-propylimidazolium bis(trifluoromethylsulfonyl)imide; [C_4mim][Tf_2N], 1-butyl-3-methylimidazolium bis(trifluoromethylsulfonyl)imide; [C_5mim][Tf_2N], 1-methyl-3-pentylimidazolium bis(trifluoromethylsulfonyl)imide; [C_6mim][Tf_2N], 1-hexyl-3-methylimidazolium bis(trifluoromethylsulfonyl)imide; [C_7mim][Tf_2N], 1-heptyl-3-methylimidazolium bis(trifluoromethylsulfonyl)imide; [C_8mim][Tf_2N], 1-octyl-3-methylimidazolium bis(trifluoromethylsulfonyl)imide; [C_4mim][PF_6], 1-butyl-3-methylimidazolium hexafluorophosphate; [C_6mim][PF_6], 1-butyl-3-hexylimidazolium hexafluorophosphate; [C_8mim][PF_6], 1-octyl-3-methylimidazolium hexafluorophosphate; [C_4C_1mim][PF_6], 1-butyl-2,3-dimethylimidazolium hexafluorophosphate; [C_4mim][BF_4], 1-butyl-3-methylimidazolium tetrafluoroborate; [C_4mim][I], 1-butyl-3-methylimidazolium iodate; [C_1mim][$(CH_3)_2PO_4$], 1,3-dimethylimidazolium dimethylphosphate; [C_2mim][$EtSO_4$], 1-ethyl-3-methylimidazolium ethylsulfate; [C_3mpy][Tf_2N], 1-*n*-propyl-3-methylpyridinium bis(trifluoromethylsulfonyl)imide; [C_3mpyr][Tf_2N], 1-methyl-1-propylpyrrolidinium bis(trifluoromethylsulfonyl)imide; [C_4mpyr][Tf_2N], 1-butyl-1-methylpyrrolidinium bis(trifluoromethylsulfonyl)imide.

* Corresponding author. Tel.: +351 234 370200; fax: +351 234 370084.
E-mail address: jcoutinho@ua.pt (J.A.P. Coutinho).

0378-3812/$ – see front matter © 2008 Elsevier B.V. All rights reserved.
doi:10.1016/j.fluid.2008.04.009

On the other hand, it was already shown that the presence of water in the IL phase can dramatically affect their pure physical properties such as viscosities, densities and surface tensions [6–9], and can acts as a co-solvent or anti-solvent in alcohols–ILs or gases–ILs systems, respectively [10–12].

One of the main ILs intrinsic attributes is the potential of tuning their physical and chemical properties and their solvating ability by varying different features of their structure, including the cation family, the cation alkyl chain length and number of alkyl groups, and the anion identity. At present, measurements on solubility and phase equilibrium of ILs and water are limited and just a few systematic studies changing the cation and/or the anion along with a temperature dependence have been attempted [13–15]. To our knowledge, other studies on both LLE and VLE water–IL systems have also been reported [3,7,10,16–32].

As it is unfeasible to experimentally measure all the possible combinations of anions and cations in ILs vapour–liquid equilibria (VLE) and liquid–liquid equilibria (LLE) systems, it is essential to make measurements on selected systems to provide results that can be used to develop correlations and to test predictive methods. Several models have been used for correlating experimental data of phase equilibria with ILs systems. Based on excess free Gibbs energy models, Wilson, UNIQUAC and original and modified UNIFAC equations have been applied to correlate solid–liquid equilibria (SLE) and VLE of ILs systems [23,33–37]. In particular, original and modified UNIFAC was also applied to correlate activity coefficients at infinite dilution and excess molar enthalpies of systems involving ILs [36]. Another local composition model that proved being able to correlate data of ILs systems was the non-random two-liquid (NRTL) that was applied to VLE and LLE systems [27,35,38–45]. Nonetheless, correlations and group-contribution methods (GCMs) are not a good option due to the lack of a sufficiently large bank of experimental data for systems involving ILs at present. The use of equations of state (EoS) requires critical parameters of the IL, which can only be obtained indirectly and with large uncertainties [8,46–48]. Nevertheless, on the basis of unimolecular quantum calculations of the individual molecules, the conductor-like screening model for real solvents (COSMO-RS) [49–51] appears to be a novel method for the prediction of thermophysical properties of fluids and can be considered as an alternative to the structure-interpolating GCMs. The COSMO-RS is also based on a physically founded model, but unlike GCMs, uses only element-specific parameters. This method is therefore, at least qualitatively, able to describe structural variations correctly.

There are few previous contributions reported in literature that deal with the application of COSMO-RS for the description of LLE systems involving ILs and alcohols, hydrocarbons, ethers or ketones [52–57]. In addition, the VLE binary systems description of ILs and alcohols, hydrocarbons, ketones or water using COSMO-RS and COSMO-RS(Ol) was merely carried by Kato and Gmehling [36], Banerjee et al. [25,26] and also by our group [13,14,57].

Thus, the goal of the present study is to evaluate the COSMO-RS potential for the prediction of the thermodynamic behaviour of systems of several nature-based ILs and water. The main ambition is to determine the impact of different ILs characteristics and the possibility to design a solvent for a specific application, in this case to fine-tune a particular IL, and with known mutual solubilities with water.

2. Phase equilibria prediction of systems involving ILs and water

Traditional approaches for correlating or predicting the properties of fluid mixtures such as EoS methods and schemes based primarily on dividing the molecules into various groups (GCMs) require a large bank of experimental data prior to their application. At present the major requirement is a predictive method that could screen the huge number of possible combinations of ILs and their mixtures, in this study with water, prior to making extensive experimental measurements.

The COSMO-RS is a unique method for predicting the thermodynamic properties of mixtures on the basis of unimolecular quantum chemical calculations for the individual molecules. COSMO-RS combines the electrostatic advantages and the computational efficiency of the quantum chemical dielectric continuum solvation model COSMO with a statistical thermodynamics approach, based on the results of the quantum chemical calculations [49–51]. The standard procedure of COSMO-RS calculations consists in two major steps: quantum chemical COSMO calculations for the molecular species involved and COSMO-RS statistical calculations performed within the COSMOtherm program [58,59].

The quantum chemical model COSMO is an efficient variant of dielectric continuum solvation methods. In these calculations the solute molecules are assumed to be in a virtual conductor environment, where the solute induces a polarization charge density, σ, on the interface between the molecule and the conductor, that is, on the molecular surface. These charges act back on the solute and give rise to a more polarized electron density than in vacuum. During the quantum chemical self-consistency cycle, the solute molecule is thus converged to its energetically optimal state in a conductor with respect to electron density, and that molecular geometry can be optimized using conventional methods for calculations in vacuum. Although time-consuming, one advantage of this procedure is that the quantum chemical calculations have to be performed just once for each molecule or ion of interest.

The COSMO-RS calculation procedure, performed using the COSMOtherm program [58,59] describes all the interactions between molecules as contact interactions of the molecular surfaces, and these interactions can be related to the screening charge densities, σ and σ', of the interacting surface pieces. The COSMO output provides the total energy of a molecule in its conductor environment and the 3D polarization density distribution on the surface of each molecule X_i. This information acts as an input for the statistical thermodynamic calculations therein after and it is independent of the solvent dielectric constant and temperature. In the COSMO-RS procedure the 3D polarization density distribution is then converted into a distribution function, the σ-profile, $p^{X_i}(\sigma)$. This last parameter describes the polarity of each surface segment on the overall surface of the molecule and quantifies the interactions of pairwise interacting surface segments in respect to the most important molecular interaction modes. If a mixture is considered, the σ-profile of a solvent S, $p_S(\sigma)$, is the result of adding the individual $p^{X_i}(\sigma)$ weighed by their mole fractions, x_i. Nevertheless, for the statistical thermodynamics of the molecular interactions is convenient to consider a normalised ensemble and since the integral of $p^{X_i}(\sigma)$ over the entire σ-range is the total surface area A^{X_i} of a compound X_i, the normalised σ-profile, $p'_S(\sigma)$, of the overall system is defined accordingly to the following equation:

$$p'_S(\sigma) = \frac{p_S(\sigma)}{A_S} = \frac{p_S(\sigma)}{\sum_{i \in S} x_i A^{X_i}} \quad (1)$$

The electrostatic misfit energy (E_{misfit}) and hydrogen bonding free energy (E_{HB}) are described as functions of the polarization charges of the two interacting segments, σ and σ' or $\sigma_{acceptor}$ and σ_{donor}, if the segments are located in a hydrogen bond donor or acceptor atom, as described in Eqs. (2) and (3). The van der Waals energy (E_{vdW}) is dependent only on the atoms involved and is

described in Eq. (4).

$$E_{\text{misfit}}(\sigma,\ \sigma') = a_{\text{eff}}\frac{\alpha'}{2}(\sigma+\sigma')^2 \quad (2)$$

$$E_{\text{HB}} = a_{\text{eff}}c_{\text{HB}}\min(0;\min(0;\sigma_{\text{donor}}+\sigma_{\text{HB}})\max(0;\sigma_{\text{acceptor}}-\sigma_{\text{HB}})) \quad (3)$$

$$E_{\text{vdW}} = a_{\text{eff}}(\tau_{\text{vdW}}+\tau'_{\text{vdW}}) \quad (4)$$

where α' is the coefficient for electrostatic misfit interactions, a_{eff} is the effective contact area between two surface segments, c_{HB} is the coefficient for hydrogen bond strength, σ_{HB} is the threshold for hydrogen bonding and τ_{vdW} and τ'_{vdW} are element-specific vdWs coefficients [51,60].

The most significant descriptor used in COSMO-RS is the local screening charge density, σ, which would be induced on the molecular surface if the molecule would be embedded in a virtual conductor. This σ descriptor is thus the key role for describing the local polarity of molecular surface and it is the only descriptor determining the interaction energies, replacing the empirical interaction parameters usually used in chemical engineering models like UNIQUAC and UNIFAC.

Thus, in COSMO-RS, the ensemble of surface pieces characterizing a liquid system S is described by the distribution function, $p_S(\sigma)$, that portrays the amount of surface in the ensemble having a screening charge density between σ and $\sigma + d\sigma$. The σ-profile of a single compound is derived from the quantum chemical COSMO output for that molecule, applying some local averaging algorithm that take into account that only screening charge densities averaged over an effective contact area are of physical meaning in COSMO-RS [51,60]. Furthermore, COSMO-RS performs the statistical thermodynamic calculations and hence yields enthalpic and entropic information for each system.

The COSMO-RS method depends only on a small number of general or at most element-specific adjustable parameters (predetermined from known properties of a small set of molecules) and that are not specific for functional groups or type of molecules. Moreover, statistical thermodynamics enables the determination of the chemical potential of all components in the mixture and, from these, the LLE, VLE and other thermodynamic properties of any mixture can be derived.

In the particular case involving ILs, a pseudobinary approach was used in the COSMOtherm program to calculate the LLE and VLE of a mixture composed of an IL and water, with the cation and anion of the IL input as separate compounds with the same mole fraction during all the procedure. The chemical potentials were calculated for the ternary system (anion + cation + water) with the chemical potential of the IL as the sum of the chemical potentials of both the cation and anion. For the case of LLE, a numerical approach was used to find the two compositions having equal chemical potentials of the three components (in the pseudobinary system) in the two phases at a particular temperature. Nevertheless, it should be noted that COSMO-RS is not able, at present, to treat ions correctly at finite low ionic strength due to the long-range ion–ion interactions involved. Thus, more experimental and theoretical work is still in need to improve the LLE and VLE predictions for systems involving ILs ions [51].

The calculation procedure and basis set parameterization of COSMO-RS calculations were done at the BP/TZVP level (Turbomole [61,62], DFT/COSMO calculation with the BP functional and TZVP [63] basis set using the fully optimized geometries at the same level of theory) and parameter file BP_TZVP_C21_0025.

3. LLE and VLE experimental database

LLE experimental data between water and imidazolium, pyridinium and pyrrolidinium-based ILs were taken from literature [13,14,22] for the following ILs: [C_4mim][BF_4], [C_4mim][PF_6], [C_6mim][PF_6], [C_8mim][PF_6], [C_4C_1mim][PF_6], [C_2mim][Tf_2N], [C_3mim][Tf_2N], [C_4mim][Tf_2N], [C_5mim][Tf_2N], [C_6mim][Tf_2N], [C_7mim][Tf_2N], [C_8mim][Tf_2N], [C_3mpy][Tf_2N], [C_3mpyr][Tf_2N] and [C_4mpyr][Tf_2N]. Further details about the experimental procedure and respective results and accuracy can be found elsewhere [13,14,22].

VLE experimental isothermal data between water and imidazolium-based ILs were taken from literature for the following ILs: [C_4mim][I], [C_4mim][BF_4], [C_4mim][PF_6], [C_8mim][PF_6], [C_2mim][Tf_2N], [C_4mim][Tf_2N], [C_1mim][$(CH_3)_2PO_4$] and [C_2mim][$EtSO_4$] [16,20,29,36].

4. Results and discussion

Prior to extensive comparisons between COSMO-RS predictions and the experimental data available, a study concerning different energy conformers of both cations and anions was performed to access the best conditions of the COSMO-RS predictions in regard to the experimental data. All the COSMO-RS calculations were carried at the BP/TZVP level (Turbomole [61,62], DFT/COSMO calculation with the BP functional and TZVP [63] basis set using the optimized geometries at the same level of theory) with the parameter file BP_TZVP_C21_0105. Therefore, the effect of the cation family, cation alkyl chain length, methyl inclusion, anion identity and temperature dependence in both LLE and VLE systems are presented and discussed.

4.1. Conformers influence

A molecule prefers to occupy the states of the low total energy and arranges its atoms accordingly. By rotation around single bonds, molecules with the same molecular formula can form geometrical isomers by arranging their atoms in different, non-equivalent positions to each other, the so-called local energy conformations or meta-stable conformations. The ions molecular geometry is optimized in vacuum and thus converged to its energetically optimal state in a conductor with respect to electron density. There are different energy states for the various conformers in the alkyl chains of [$C_n$mim] and [$C_n$pyr] cations and in the [Tf_2N] and [$(CH_3)_2PO_4$] anions studied. Thus it is important from a theoretical point of view to evaluate the effect of the various conformers on the predicted LLE and VLE systems. To study the influence of the ILs conformations on the COSMO-RS predictions, the meta-stable conformations with the lowest and higher COSMO energies have been tested. The global minimum energy conformations for ILs consist of the geometrically optimized minimum energy structure for both the cation and the anion and the local minima energy conformations consist in meta-stable conformations but with higher potential energy surfaces than the global minimum. Besides the [Tf_2N] and [$(CH_3)_2PO_4$] anions that were found to have two and three stable conformers each, in some cases just the effect of the cation is studied, because only one structure of the anions [I], [$EtSO_4$], [BF_4] and [PF_6] was found. Some examples of the conformers influence results are depicted in Figs. 1–3, both in the LLE and VLE phase diagrams.

The results presented in Fig. 1 show that different cation energy conformations have a small effect on the predicted mutual solubilities, and similar behaviours in the LLE study were obtained for other cations family-based and other cations alkyl chain length examples. Nevertheless, higher deviations are found for the [C_4mim][Tf_2N] and water phase diagram presented in Fig. 2, where besides the presence of the cation conformers, the anion also presents two different local minima energy geometrical isomers. There is a combination of minimal energy conformations of both cation and anion,

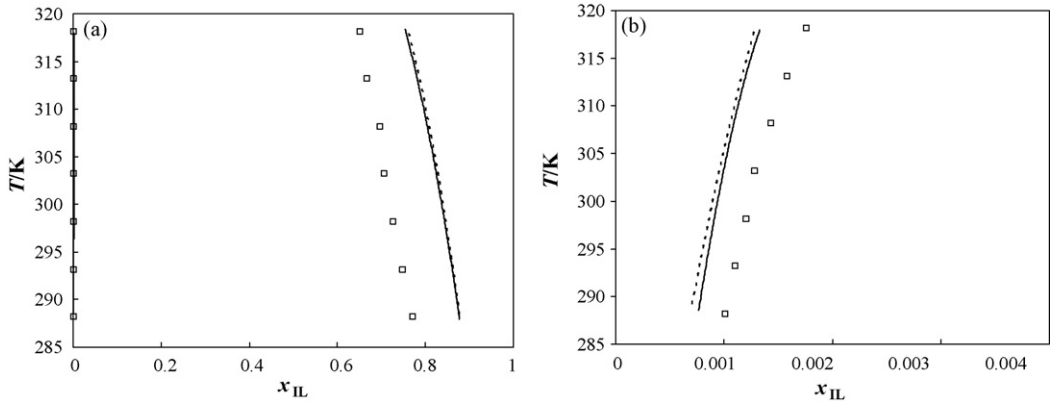

Fig. 1. Complete liquid–liquid phase diagram for water and [C_4mim][PF_6] (a) and water-rich phase side (b): (□) experimental data; (—) COSMO-RS predictions with global minimum ion conformers; (- - -) COSMO-RS predictions with local minima ion conformers.

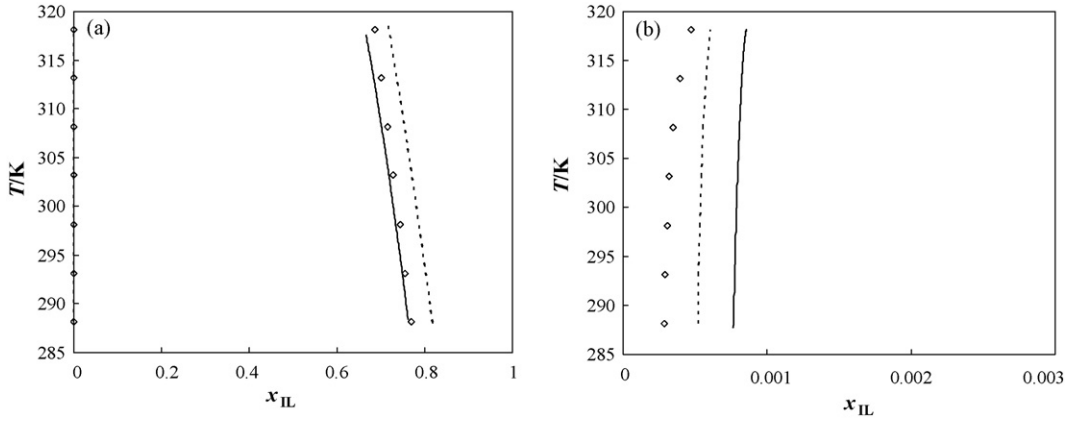

Fig. 2. Complete liquid–liquid phase diagram for water and [C_4mim][Tf_2N] (a) and water-rich phase side (b): (◊) experimental data; (—) COSMO-RS predictions with global minimum ion conformers; (- - -) COSMO-RS predictions with local minima ion conformers.

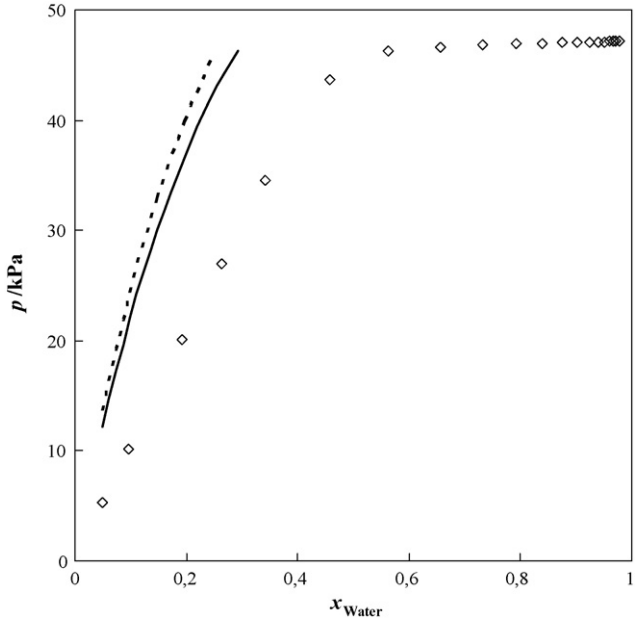

Fig. 3. Vapour–liquid phase diagram for water and [C_4mim][Tf_2N]: (◊) experimental data; (—) COSMO-RS predictions with the global minimum ion conformers; (- - -) COSMO-RS predictions with local minima ion conformers.

showing that the anion plays an important role in the H-bonding interactions with water.

One example of the diverse energy conformations influence in the [C_4mim][Tf_2N] and water VLE behaviour is presented in Fig. 3. For both vapour–liquid phase diagrams of [C_2mim][Tf_2N] and [C_4mim][Tf_2N] with water, the positive deviation from Raoult's law is predicted, and the best results in respect to experimental data are with the lowest energy conformation ions. Nevertheless, smaller differences due to the ions conformers are obtained in the VLE studies because of the ILs negligible vapour pressures and their small contribute in this type of phase behaviour.

In both LLE and VLE studies the best predictions in respect to experimental data are obtained with the lowest energy conformations or with the global minimum for both cation and/or anion. This trend is observed for almost all the binary systems analysed and thus the lowest energy isomers conformation for all the species involved will be used in the COSMO-RS calculations below.

4.2. Liquid–liquid equilibria predictions

Using the optimal global minimum energy ions conformers, the phase diagram for a number of binary IL–water systems was predicted. In this part of the work the quantum chemical COSMO calculations for the ILs under study were performed with the Turbomole program package [61,62] using the BP density functional

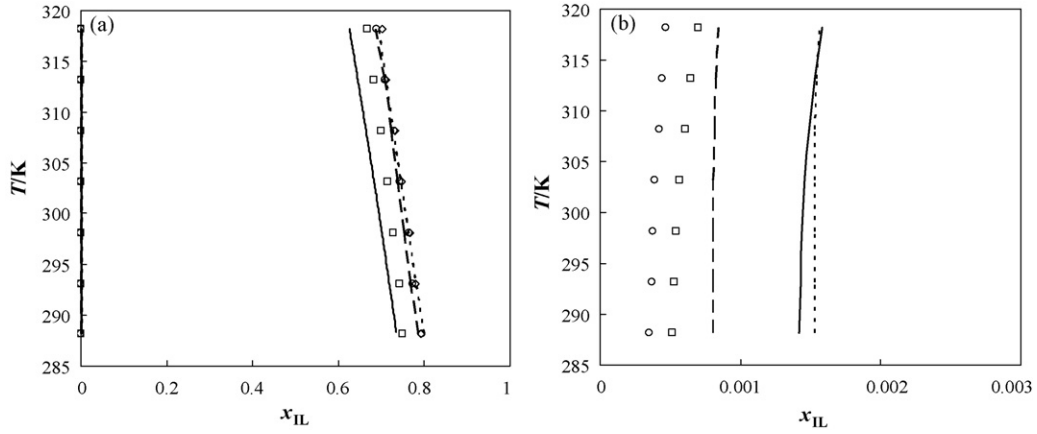

Fig. 4. Complete liquid–liquid phase diagram for water and ILs (a) and water-rich phase side (b): (□) (—) [C_3mim][Tf_2N]; (○) (— —) [C_3py][Tf_2N]; (◊) (- - -) [C_3pyr][Tf_2N]. The single symbols and the lines represent, respectively the experimental data and the COSMO-RS predictions.

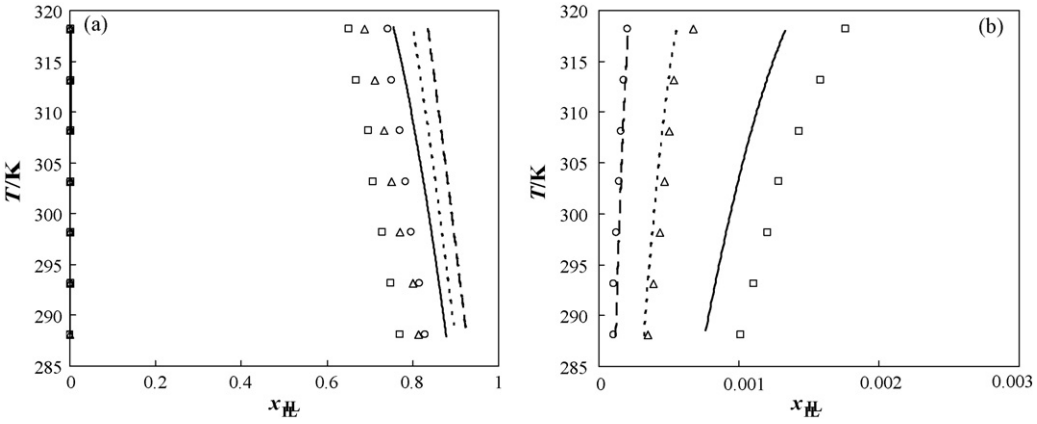

Fig. 5. Complete liquid–liquid phase diagram for water and ILs (a) and water-rich phase side (b): (□) (—) [C_4mim][PF_6]; (△) (- - -) [C_6mim][PF_6]; (○) (— —) [C_8mim][PF_6]. The single symbols and the lines represent, respectively the experimental data and the COSMO-RS predictions.

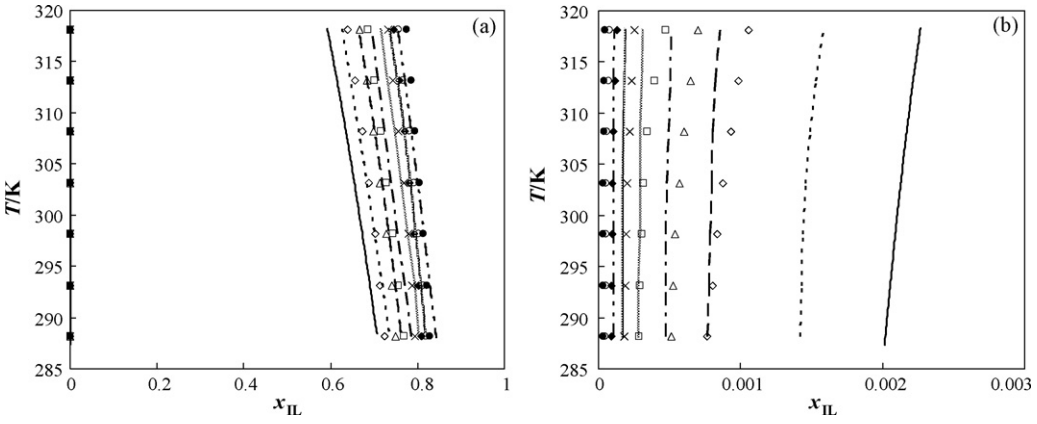

Fig. 6. Complete liquid–liquid phase diagram for water and ILs (a) and water-rich phase side (b): (◊) (—) [C_2mim][Tf_2N]; (△) (- - -) [C_3mim][Tf_2N]; (□) (— —) [C_4mim][Tf_2N]; (×) (— - —) [C_5mim][Tf_2N]; (♦) (▬▬▬▬▬▬) [C_6mim][Tf_2N]; (○) (▪▪▪▪▪▪▪▪▪▪▪▪) [C_7mim][Tf_2N]; (●) (— - - —) [C_8mim][Tf_2N]. The single symbols and the lines represent, respectively the experimental data and the COSMO-RS predictions.

theory and the triple-ζ valence polarized large basis set (TZVP) [63]. These calculations were made for a true three-component mixture where the cation and anion of equal mole fractions were treated as separate species. Experimental data in the form of T–x_{IL} for each binary mixture investigated and the results obtained with the COSMO-RS predictive calculations are compared in Figs. 4–9.

The ILs–water systems studied present an asymmetric LLE behaviour due to the higher solubility of water in ILs while their solubility in water is very small. In fact, the mole fraction solubility of the studied ILs in water ranges from 3.4×10^{-5}, for the [C_8mim][Tf_2N], to complete miscibility at room temperature, for [C_4mim][BF_4]. On the other hand, the mole fractions solubilities of

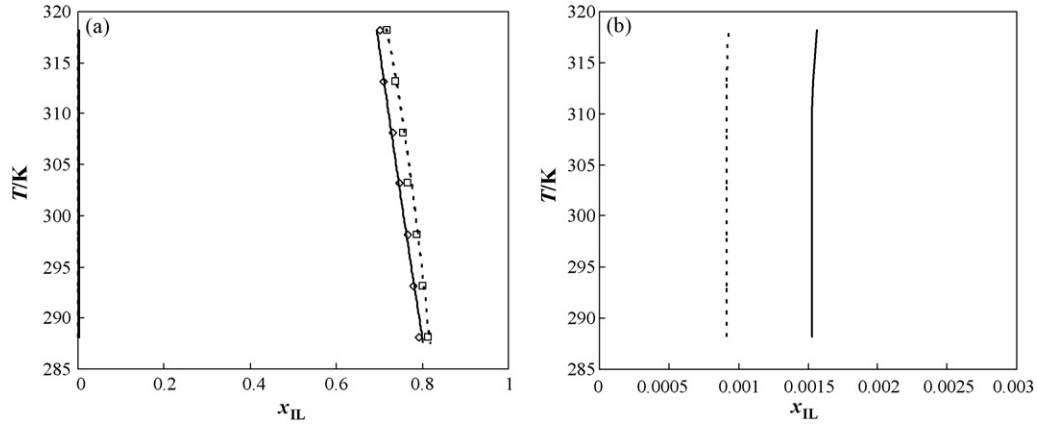

Fig. 7. Complete liquid–liquid phase diagram for water and ILs (a) and water-rich phase side (b): (◊) (—) [C_3mpyr][Tf_2N]; (□) (- - -) [C_4mpyr][Tf_2N]. The single symbols and the lines represent, respectively the experimental data and the COSMO-RS predictions.

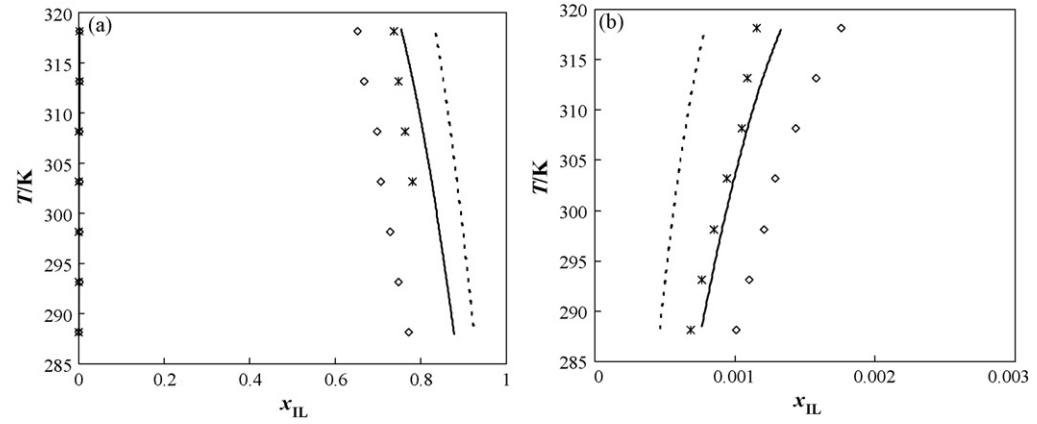

Fig. 8. Complete liquid–liquid phase diagram for water and ILs (a) and water-rich phase side (b): (◊) (—) [C_4mim][PF_6]; (*) (- - -) [C_4C_1mim][PF_6]. The single symbols and the lines represent, respectively the experimental data and the COSMO-RS predictions.

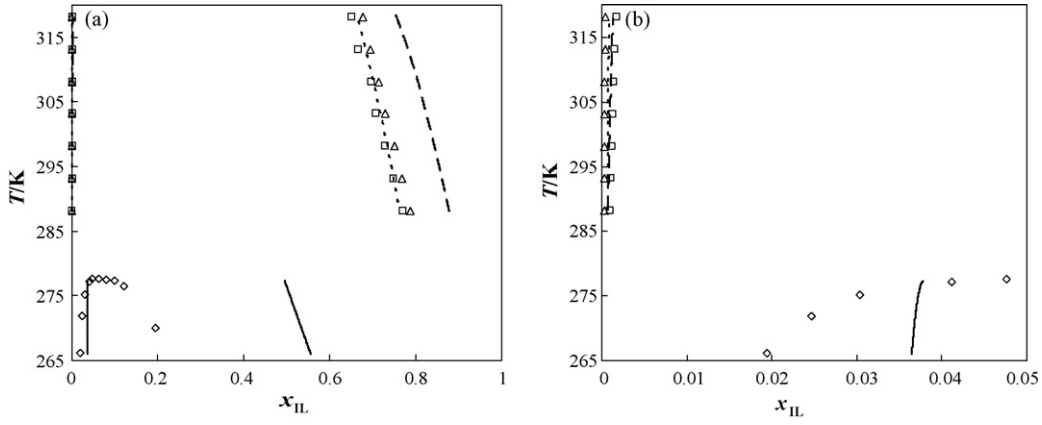

Fig. 9. Complete liquid–liquid phase diagram for water and ILs (a) and water-rich phase side (b): (◊) (—) [C_4mim][BF_4]; (□) (— —) [C_4mim][PF_6]; (△) (- - -) [C_4mim][Tf_2N]. The single symbols and the lines represent, respectively the experimental data and the COSMO-RS predictions.

water in the ILs studied range from 0.19 to the complete miscibility, at room temperature, and depend on both the cation and the anion identity. However, since the main goal of this work is to study the impact of the ILs anions and cations structural variations on the predicted phase diagrams the mole fraction basis was adopted.

The results obtained are discussed below from different perspectives to evaluate the impact of ILs structural variations on the COSMO-RS predictive capability for mutual solubilities with water.

4.2.1. Cation class influence

The influence of different cations family on IL–water LLE systems can be assessed by examination of the experimental phase diagrams of imidazolium, pyridinium and pyrrolidinium-based ILs in combination with the common anion [Tf_2N] [13,14], as well as their predictions using COSMO-RS, presented in Fig. 4. Due to the asymmetrical character of the LLE behaviour the figures present both the general LLE diagrams and the water-rich side of the equilibrium.

The overall trend is well predicted with the hydrophobic tendency increasing from [C_3mim] < [C_3mpy] < [C_3mpyr] as verified experimentally for the IL-rich phase. Besides the qualitative description, the predictions also provide a good quantitative description of the experimental data. For the water-rich phase the predictive hydrophobic tendency is also well described.

In general, it seems that the COSMO-RS is able to describe well, both qualitatively and quantitatively, water–IL LLE systems based on extremely hydrophobic anions, as the case of [Tf_2N]-based anions, and independently of the cation class or the cation hydrophobicity.

4.2.2. Cation alkyl chain length influence

Figs. 5–7 show the liquid–liquid experimental data [13,14] and the predicted phase behaviour with water for two anions, [PF_6] and [Tf_2N], in combination with different alkyl chain length imidazolium and pyrrolidinium-based ILs.

The influence of the cation alkyl chain length on the mutual solubilities appeared to follow the same trend with both the anions and cations families, where there is an increase in the IL hydrophobic character with the cation alkyl chain length increase. That hydrophobic tendency occurs at both sides of the equilibrium but plays a major role on the water-rich side, where differences of one order of magnitude appear when comparing the solubility of [C_4mim][PF_6] with [C_8mim][PF_6] and even of two orders of magnitude comparing [C_2mim][Tf_2N] with [C_8mim][Tf_2N] in water at room temperature.

The results obtained from COSMO-RS calculations show an acceptable agreement with the experimental data available, and follow the ILs hydrophobic character increase with the cation alkyl chain length increase, depicting the good qualitatively prediction capacity of this method. Higher relative deviations between experimental data and COSMO-RS predictions were found in the water-rich phase, but it should be mentioned that the ILs solubility in water can be considered as to being at infinite dilution and that predictions can always be considered reasonable satisfactory at the quantitative level.

It is interesting to note that the liquid–liquid phase behaviour between alcohols and ILs follows the opposite trend of that observed for water–ILs systems. The higher the alkyl side chain length of the cation the higher are the mutual solubilities between alcohols and ILs essentially due to the increase in the van der Waals interactions. In both cases COSMO-RS seems to be able to correctly describe the mutual solubilities changes induced by the cation alkyl side chain length increase [57].

4.2.3. Cation methyl inclusion influence

Fig. 8 presents the comparison between water and [C_4mim][PF_6] or [C_4C_1mim][PF_6] mutual solubilities for both experimental and COSMO-RS predictive results [13,14].

By replacing the hydrogen of the [C_4mim] cation at the C2 position with a methyl group (forming [C_4C_1mim]) the ability of the cation to hydrogen bond with water is greatly diminished, resulting in a decrease in the mutual solubilities between the previous imidazolium-based IL and water. Clearly, hydrogen bonding of water with the most acidic hydrogen of the imidazolium cation has some influence in controlling liquid–liquid phase behaviour between imidazolium-based ILs and water. COSMO-RS calculations agree well with experimental results for both sides of the equilibrium predicting correctly the IL hydrophobic character increase and the variation in mutual solubilities due to a methyl inclusion at the imidazolium cation.

4.2.4. Anion identity

Fig. 9 shows the comparison between the experimental data [13,14,22] and COSMO-RS predictions using the BP/TZVP procedure for the liquid–liquid phase behaviour of the [C_4mim] cation in combination with three different anions: [BF_4], [PF_6] and [Tf_2N].

In the water-rich phase COSMO-RS proved to predict the increase in the hydrophobicity nature due to the anion identity from [BF_4] < [PF_6] < [Tf_2N], following the experimental mutual solubilities decrease with water. However, in the IL-rich phase the IL hydrophobic tendency between [PF_6] and [Tf_2N] is not well described when compared to the experimental data. COSMO-RS predicts a higher solubility of water in [C_4mim][Tf_2N] than in [C_4mim][PF_6], may be due to the fact that the [Tf_2N] is a stronger Lewis base than [PF_6]. Conversely, [PF_6] has a greater charge density than [Tf_2N] because it is smaller, so it can have stronger Coulombic interactions. Clearly the phase behaviour is the result of several competing interactions in the solution and all types of interactions should be considered. Moreover it was demonstrated that both the cation and anion affect the mutual solubilities, but from Fig. 9, it is the anion that plays the major role on the phase behaviour of imidazolium-based ILs with water. Thus, changing the anion is the easiest way to adjust the liquid–liquid equilibrium with water.

A good quantitative general description was found for [C_4mim][Tf_2N]–water system over the entire liquid–liquid phase diagram. In fact, and as stated before, for the cation family influence study it seems that the COSMO-RS is capable of describing improved systems with extremely hydrophobic anions than those based in more hydrophilic anions, as [BF_4] and [PF_6]. The predictions show a clear quantitative degradation with the anion hydrophilic character increase.

In general, the predictive LLE capacity of COSMO-RS seems to improve with the increasing polarity of the solvent, since better quantitative descriptions are obtained in this work for water involving systems, when compared with the COSMO-RS predictions for LLE binary systems of ILs with alcohols, alkanes and ketones where the mutual solubilities deviations were found to be larger than those reported in the present work [54–57].

From the present results and our previous contribution [57] a global remark can be established for the IL–solvent binary systems LLE predictions. It appears that the larger the difference between the IL and the solvent polarity, the better are the quantitative and qualitative predictions. For IL–water systems the predictions start to deviate with the anion hydrophilic nature increase, while for IL–alcohol systems the predictions start to deviate with both the cation alkyl side chain and alcohol chain length increase.

4.3. Vapour–liquid equilibria predictions

The vapour-phase behaviour for several IL–water systems was available from literature [16,20,29,36] and the comparison between the COSMO-RS predictions, using the BP/TZVP procedure and the lowest energy ion conformations, with the experimental data was performed. The results are presented in Figs. 10–20 in the form of p–x_{water} data for each binary mixture investigated. Again the COSMO-RS calculations were made for a true three-component mixture where the cation and anion of equal concentrations are treated as separate species. The results obtained for the isotherms p–x_{water} phase diagrams are discussed below from different views to evaluate the influence of the ILs structural variations and its dependence with temperature and the COSMO-RS predictive capability.

4.3.1. Cation alkyl chain length influence

Figs. 10–12 show the experimental vapour–liquid phase behaviour for three anions, [BF_4], [PF_6] and [Tf_2N], in combination

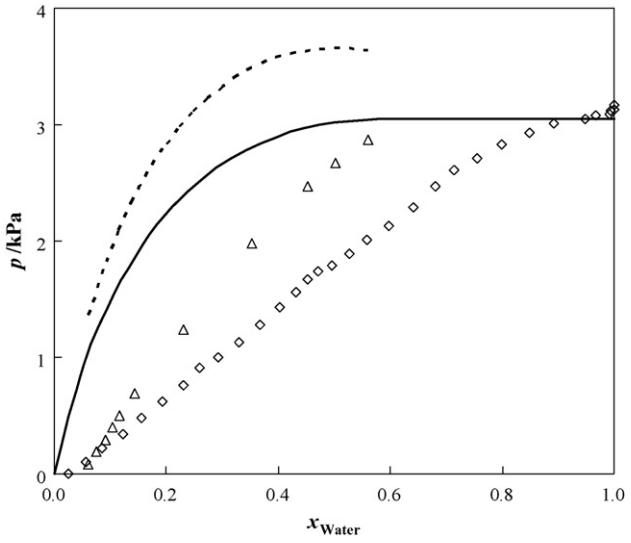

Fig. 10. Vapour–liquid phase diagram for water and ILs at 298.15 K: (◊) (—) [C_4mim][BF_4]; (△) (- - -) [C_8mim][BF_4]. The single symbols and the lines represent, respectively the experimental data and the COSMO-RS predictions.

with different alkyl chain length imidazolium-based ILs [16,20,36] and the respective comparison with the COSMO-RS prediction results.

From Figs. 10–12, COSMO-RS provides a good qualitative description of the p–x_{water} phase diagrams in respect to the cation alkyl chain length variation with the three different anions ([BF_4], [PF_6] and [Tf_2N]) when compared to the experimental data [16,20,36]. There is an increase of the positive deviation from Raoult's law and also an increase of the ILs hydrophobic nature with the alkyl chain length. However, and in accordance with the results reported for the LLE predictions, better quantitative results are obtained for water–IL systems with the hydrophobic anion [Tf_2N].

Furthermore, in Fig. 12 it is shown the occurrence of a miscibility gap with the [Tf_2N]-based ILs; this same behaviour is expected with the [PF_6]-based ILs, although the mole fraction range presented is not enough to prove this fact experimentally. Besides the positive deviation from Raoult's law that is predicted for the three anions, COSMO-RS showed to be able to give at least *a priori* good qualitative predictions.

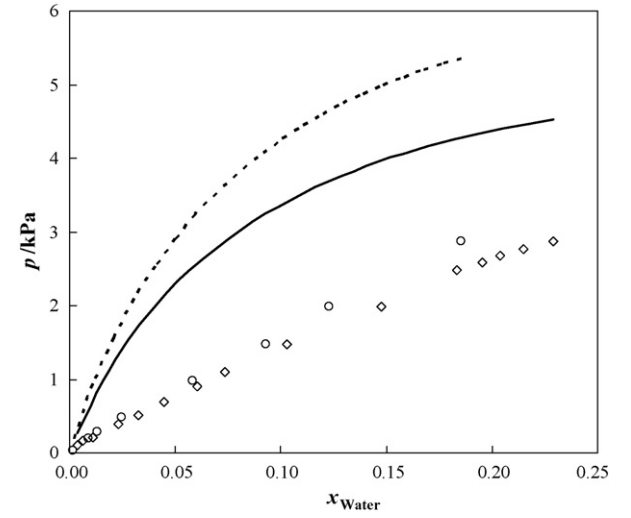

Fig. 11. Vapour–liquid phase diagram for water and ILs at 298.15 K: (◊) (—) [C_4mim][PF_6]; (○) (- - -) [C_8mim][PF_6]. The single symbols and the lines represent, respectively the experimental data and the COSMO-RS predictions.

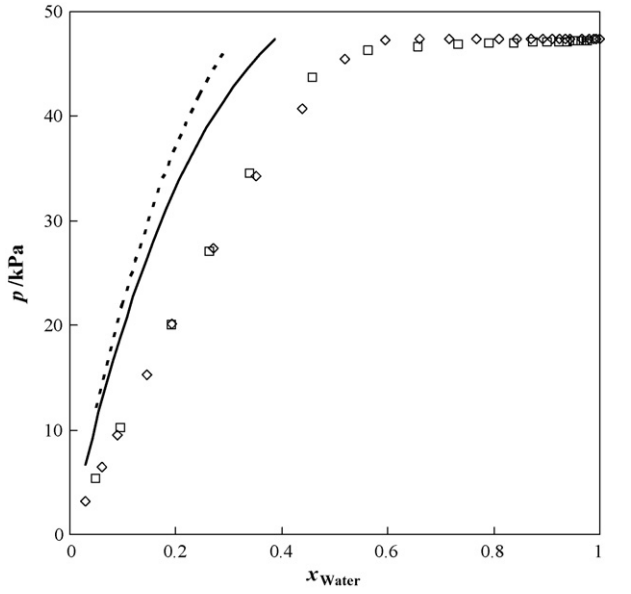

Fig. 12. Vapour–liquid phase diagram for water and ILs at 353.15 K: (◊) (—) [C_2mim][Tf_2N]; (□) (- - -) [C_4mim][Tf_2N]. The single symbols and the lines represent, respectively the experimental data and the COSMO-RS predictions.

4.3.2. Anion identity influence

Figs. 13 and 14 show the comparison between experimental data and COSMO-RS predictions using the BP/TZVP procedure for the vapour–liquid phase behaviour for the [C_8mim] cation, in combination with two anions: [BF_4] and [PF_6] [16], and for the [C_4mim] cation in combination with different anions: [BF_4] and [I] [20]. Figs. 15 and 16 present the results obtained for water with the [C_1mim][$(CH_3)_2PO_4$] and the [C_2mim][$EtSO_4$] ILs vapour–liquid phase equilibria, respectively [29,36]. However, a direct comparison with other anions cannot be made due to the lack of experimental data reporting these two anions in combination with other cations.

From the inspection of Figs. 13 and 14, the COSMO-RS proved to predict well the hydrophobic tendency increase in the vapour–liquid phase equilibria due to the anion identity from [I] < [BF_4] < [PF_6], following the same trend of the experimental data and also as verified for the LLE.

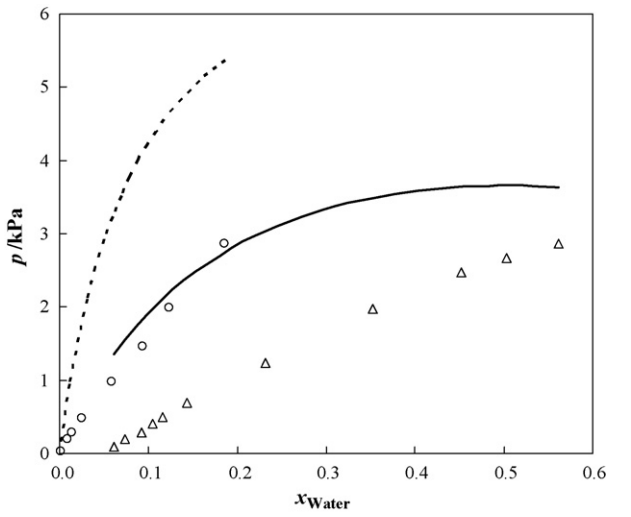

Fig. 13. Vapour–liquid phase diagrams for water and ILs at 298.15 K: (△) (—) [C_8mim][BF_4]; (○) (- - -) [C_8mim][PF_6]. The single symbols and the lines represent, respectively the experimental data and the COSMO-RS predictions.

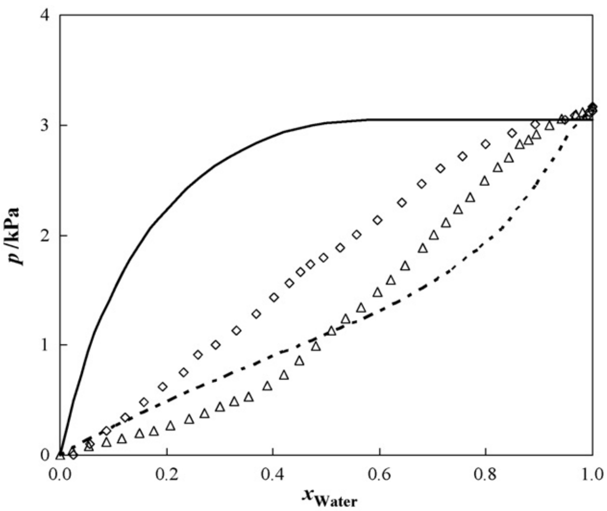

Fig. 14. Vapour–liquid phase diagram for water and ILs at 298.15 K: (◊) (—) [C_4mim][BF_4]; (△) (- - -) [C_4mim][I]. The single symbols and the lines represent, respectively the experimental data and the COSMO-RS predictions.

Moreover it was demonstrated that both the cation and anion affect the vapour–liquid phase equilibria, but comparing Figs. 13–16 it is again the anion that plays the major role on the vapour-phase behaviour of imidazolium-based ILs with water, as verified for the LLE type systems.

From Figs. 14–16, the COSMO-RS demonstrated also that it is able to describe well phase diagrams with negative deviations from Raoult's law, as experimentally evidenced for the [C_4mim][I], [C_1mim][$(CH_3)_2PO_4$] and [C_2mim][$EtSO_4$]–water binary systems.

4.3.3. Temperature dependence influence

Figs. 17–20 show the comparison between the experimental data [16,29] and COSMO-RS predictive results using the BP/TZVP procedure for the vapour–liquid phase behaviour at several isotherms for the following ILs: [C_4mim][PF_6], [C_8mim][PF_6], [C_8mim][BF_4] and [C_2mim][$EtSO_4$].

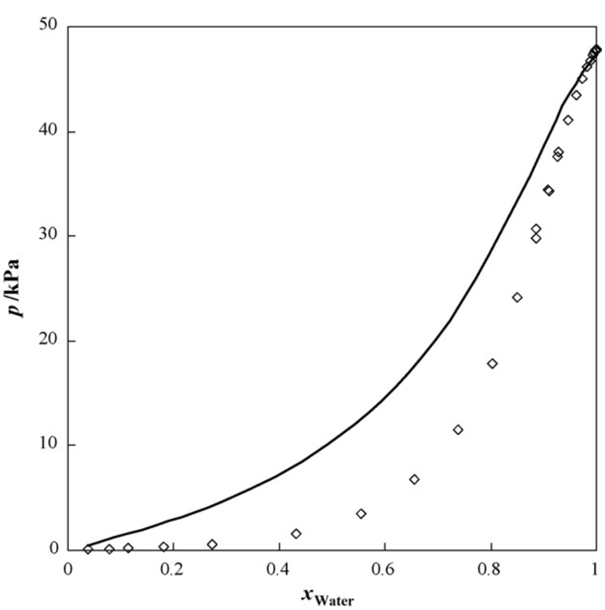

Fig. 15. Vapour–liquid phase diagram for water and [C_1mim][$(CH_3)_2PO_4$] at 353.15 K: (◊) (—). The single symbols and the lines represent, respectively the experimental data and the COSMO-RS predictions.

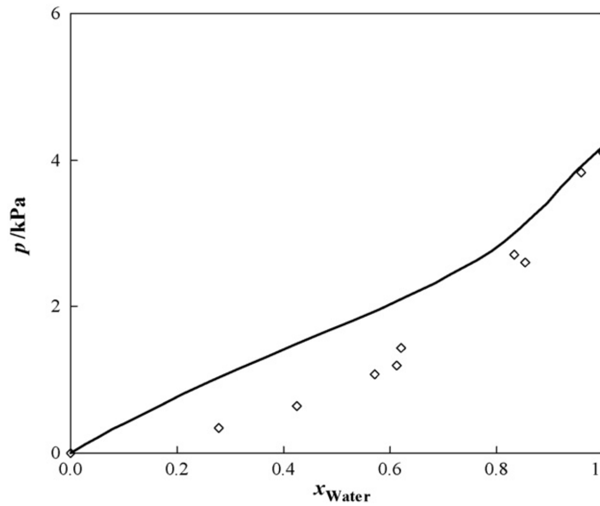

Fig. 16. Vapour–liquid phase diagram for water and [C_2mim][$EtSO_4$] at 302.19K: (◊) (—). The single symbols and the lines represent, respectively the experimental data and the COSMO-RS predictions.

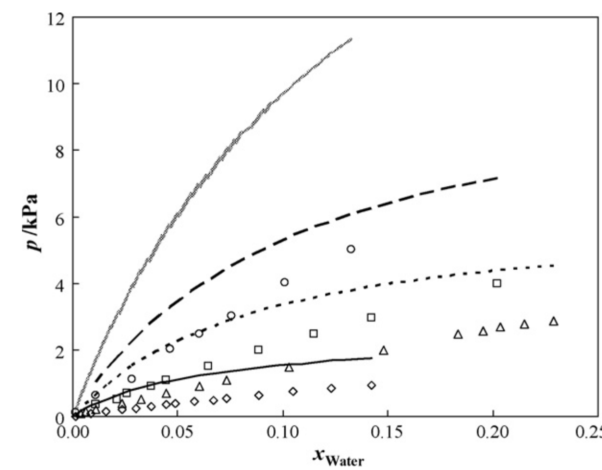

Fig. 17. Vapour–liquid phase diagrams for water and [C_4mim][PF_6] at isotherms: (◊) (—) 283.15 K; (△) (- - -) 298.15 K; (□) (— —) 308.15 K; (○) (∼∼∼∼) 323.15 K. The single symbols and the lines represent, respectively the experimental data and the COSMO-RS predictions.

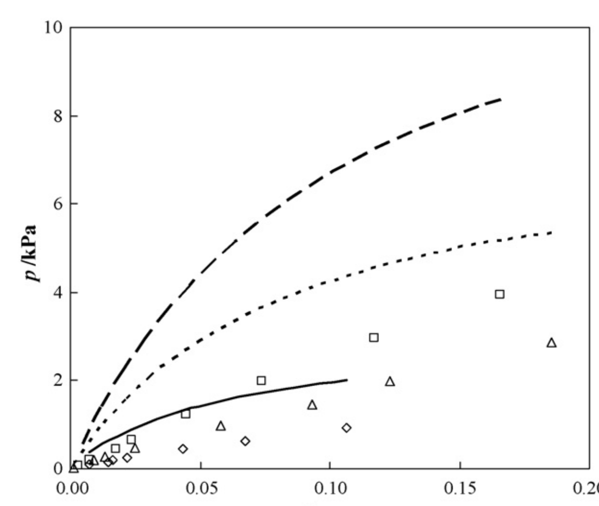

Fig. 18. Vapour–liquid phase diagram for water and [C_8mim][PF_6] at isotherms: (◊) (—) 283.15 K; (△) (- - -) 298.15 K; (□) (— —) 308.15 K. The single symbols and the lines represent, respectively the experimental data and the COSMO-RS predictions.

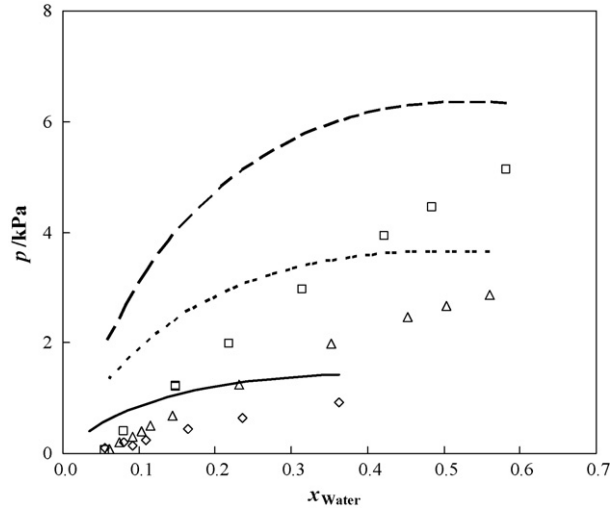

Fig. 19. Vapour–liquid phase diagram for water and $[C_8mim][BF_4]$ at isotherms: (◊) (—) 283.15 K; (△) (- - -) 298.15 K; (□) (— —) 308.15 K. The single symbols and the lines represent, respectively the experimental data and the COSMO-RS predictions.

From Figs. 17–20, COSMO-RS showed to be able to describe the vapour–liquid phase diagrams behaviour, increasing pressure with the increase of temperature as verified experimentally. Although the quantitative predictions are not perfect, the COSMO-RS was able to describe the qualitative variations due to temperature in all the ILs analysed that are composed by different cations and/or anions.

Although data in a larger temperature range would be required to fully establish the adequacy of the temperature dependence of the COSMO-RS predictions, the results here reported and along with the LLE results, seem to indicate that COSMO-RS provides a correct temperature dependence of the liquid phase non-ideality.

Comparing the LLE and VLE results, the VLE description is qualitatively superior following the same behaviour for all the ILs combinations studied when compared with experimental data. For the LLE results some improvements should be made to achieve a better description of the anion influence in the mutual solubilities between water and ILs.

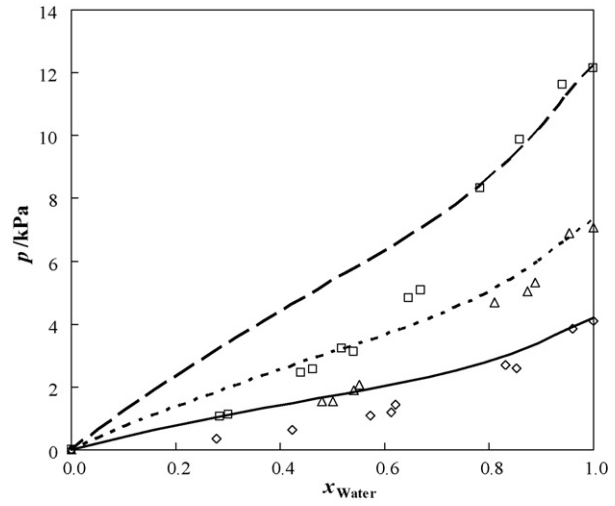

Fig. 20. Vapour–liquid phase diagram for water and $[C_2mim][EtSO_4]$ at isotherms: (◊) (—) 302.19 K; (△) (- - -) 312.19 K; (□) (— —) 322.19 K. The single symbols and the lines represent, respectively the experimental data and the COSMO-RS predictions.

5. Conclusions

ILs have been suggested as potential "green" solvents due to their negligible vapour pressures. To develop ILs as prospective solvents for diverse applications it is important to gain a fundamental understanding of the factors that control the phase behaviour of ILs with other liquids, including polar solvents as water. Since it is not feasible to experimentally determine all the possible combinations with ILs, a predictive method capable of describing the phase behaviour of such systems is of extreme importance. Quantum chemical calculations based on the σ profiles of the cation, the anion, and water were used for the prediction of LLE and VLE systems incorporating ILs and water. COSMO-RS and its implementation in the program COSMOtherm showed to be capable of giving satisfactory *a priori* qualitative predictions of the thermodynamics of systems involving ILs, which may be of considerable value for the exploration of suitable ILs for practical and specific applications.

The VLE predictions showed to be more accurate in respect to the available experimental data, describing well all the ILs structural modifications in their phase behaviour. Nevertheless, for the LLE predictions some model limitations were found, especially for the anions influence.

Although a reasonable qualitative prediction was obtained for the various ILs studied, the deviations from experimental data seem to increase with the IL anion hydrophilic character. On the other hand, the cation hydrophilic character does not lead to this deviation increase from experimental data.

List of symbols

a_{eff}	effective contact area between two surface segments
A^{X_i}	total surface area of molecule X_i
c_{HB}	hydrogen bond strength coefficient
E_{HB}	hydrogen bonding free energy
E_{misfit}	electrostatic misfit energy
E_{vdW}	van der Waals energy
p	pressure
$p_S(\sigma)$	sigma profile of a solvent
$p^{X_i}(\sigma)$	sigma profile of a solute i
$P'_S(\sigma)$	normalised sigma profile of a solvent
T	temperature
x_i	mole fraction of compound i
x_{IL}	ionic liquid mole fraction
X_i	i molecule considered as solute

Greek symbols

α'	electrostatic misfit interactions coefficient
σ	polarization charge density
$\sigma_{acceptor}$	polarization charge of a hydrogen
σ_{donor}	polarization charge of a hydrogen bonding donor
σ_{HB}	hydrogen bonding threshold bonding acceptor
τ_{vdW}	element-specific vdWs coefficient
τ'_{vdW}	element-specific vdWs coefficient

Acknowledgments

The authors thank financial support from Fundação para a Ciência e a Tecnologia (Project POCI/EQU/58152/2004) and Ph.D. grant (SFRH/BD/14134/2003) of Mara G. Freire. They also acknowledge F. Eckert and A. Klamt, COSMOtherm, Version C2.1, Release 01.05, COSMOlogic GmbH & Co. KG, Leverkusen, Germany, 2005, and M. Diedenhofen of COSMOlogic for advice and assistance in the use of COSMOtherm.

References

[1] J.G. Huddleston, H.D. Willauer, R.P. Swatloski, A.E. Visser, R.D. Rogers, Chem. Commun. 44 (1998) 1765–1766.
[2] A.G. Fadeev, M.M. Meagher, Chem. Commun. 44 (2001) 295–296.
[3] J. McFarlane, W.B. Ridenour, H. Luo, R.D. Hunt, D.W. DePaoli, D.W.R.X. Ren, Sep. Sci. Technol. 40 (2005) 1245–1265.
[4] J. Ranke, A. Müller, U. Bottin-Weber, F. Stock, S. Stolte, J. Arning, R. Störmann, B. Jastorff, Ecotoxicol. Environ. Saf. 67 (2007) 430–438.
[5] D. Zhao, Y. Liao, Z. Zhang, Clean 35 (2007) 42–48.
[6] K.R. Seddon, A. Stark, M.-J. Torres, Pure Appl. Chem. 72 (2000) 2275–2287.
[7] J.G. Huddleston, A.E. Visser, W.M. Reichert, H.D. Willauer, G.A. Broker, R.D. Rogers, Green Chem. 3 (2001) 156–164.
[8] M.G. Freire, P.J. Carvalho, A.M. Fernandes, I.M. Marrucho, A.J. Queimada, J.A.P. Coutinho, J.Colloid Interface Sci. 314 (2007) 621–630.
[9] R.L. Gardas, M.G. Freire, P.J. Carvalho, I.M. Marrucho, I.M.A. Fonseca, A.G.M. Ferreira, J.A.P. Coutinho, J. Chem. Eng. Data 52 (2007) 80–88.
[10] V. Najdanovic-Visak, J.M.S.S. Esperança, L.P.N. Rebelo, M. Nunes da Ponte, H.J.R. Guedes, K.R. Seddon, J. Szydlowskiy, Phys. Chem. Chem. Phys. 4 (2002) 1701–1703.
[11] V. Najdanovic-Visak, L.P.N. Rebelo, M. Nunes da Ponte, Green Chem. 7 (2005) 443–450.
[12] S.P.M. Ventura, J. Pauly, J.L. Daridon, J.A. Lopes da Silva, I.M. Marrucho, A.M.A. Dias, J.A.P. Coutinho, J. Chem. Thermodyn. (2008), in press, doi:10.1016/j.jct.2008.04.012.
[13] M.G. Freire, C.M.S.S. Neves, P.J. Carvalho, R.L. Gardas, A.M. Fernandes, I.M. Marrucho, L.M.N.B.F. Santos, J.A.P. Coutinho, J. Phys. Chem. B 111 (2007) 13082–13089.
[14] M.G. Freire, P.J. Carvalho, R.L. Gardas, I.M. Marrucho, L.M.N.B.F. Santos, J.A.P. Coutinho, J. Phys. Chem. B 112 (2008) 1604–1610.
[15] M.G. Freire, L.M.N.B.F. Santos, A.M. Fernandes, J.A.P. Coutinho, I.M. Marrucho, Fluid Phase Equilib. 261 (2007) 449–454.
[16] J.L. Anthony, E.J. Maggin, J.F. Brennecke, J. Phys. Chem. B 105 (2001) 10942–10949.
[17] D.S.H. Wong, J.P. Chen, J.M. Chang, C.H. Chou, Fluid Phase Equilib. 194–197 (2002) 1089–1095.
[18] Z.B. Alfassi, R.E. Huie, B.L. Milman, P. Neta, Anal. Bioanal. Chem. 377 (2003) 159–164.
[19] J.M. Crosthwaite, S.N.V.K. Aki, E.J. Maggin, J.F. Brennecke, J. Phys. Chem. B 108 (2004) 5113–5119.
[20] H. Katayanagi, K. Nishikawa, H. Shimozaki, J. Phys. Chem. B 108 (2004) 19451–19457.
[21] K. Kim, S. Park, S. Choi, H. Lee, J. Chem. Eng. Data 49 (2004) 1550–1553.
[22] L.P.N. Rebelo, V. Najdanovic-Visak, Z.P. Visak, M. Nunes da Ponte, J. Szydlowski, C.A. Cerdeiriña, J. Troncoso, L. Romaní, J.M.S.S. Esperança, H.J.R. Guedes, H.C. de Sousa, Green Chem. 6 (2004) 369–381.
[23] R. Kato, J. Gmehling, Fluid Phase Equilib. 231 (2005) 38–43.
[24] N.V. Shvedene, S.V. Borovskaya, V.V. Sviridov, E.R. Ismailova, I.V. Pletnev, Anal. Bioanal. Chem. 381 (2005) 427–430.
[25] T. Banerjee, M.K. Singh, A. Khanna, Ind. Eng. Chem. Res. 45 (2006) 3207–3219.
[26] T. Banerjee, M.K. Singh, A. Khanna, Ind. Eng. Chem. Res. 45 (2006) 6876–16876.
[27] N. Calvar, B. González, E. Gómez, A. Domínguez, J. Chem. Eng. Data 51 (2006) 2178–2181.
[28] N. Papaiconomou, N. Yakelis, J. Salminen, R. Bergman, J.M. Prausnitz, J. Chem. Eng. Data 51 (2006) 1389–1393.
[29] I.A. Sumartschenkowa, S.P. Verevkin, T.V. Vasiltsova, E. Bich, A. Heintz, M.P. Shevelyova, G.J. Kabo, J. Chem. Eng. Data 51 (2006) 2138–2144.
[30] S.L.I. Toh, J. McFarlane, C. Tsouris, D.W. DePaoli, H. Luo, S. Dai, Solvent Extr. Ion Exch. 24 (2006) 33–56.
[31] U. Domańska, A. Marciniak, Green Chem. 9 (2007) 262–266.
[32] U. Domańska, I. Bakala, J. Pernak, J. Chem. Eng. Data 52 (2007) 309–314.
[33] U. Domańska, E. Bogel-Łukasik, Ind. Eng. Chem. Res. 42 (2003) 6986–6992.
[34] U. Domańska, E. Bogel-Łukasik, R. Bogel-Łukasik, Chem. Eur. J. 9 (2003) 3033–3041.
[35] M. Doker, J. Gmehling, Fluid Phase Equilib. 227 (2005) 255–266.
[36] R. Kato, J. Gmehling, J. Chem. Thermodyn. 37 (2005) 603–619.
[37] U. Domańska, Thermochim. Acta 448 (2006) 19–30.
[38] T.M. Letcher, P. Reddy, Fluid Phase Equilib. 219 (2004) 107–112.
[39] T.M. Letcher, N. Deenadayalu, B. Soko, D. Ramjugernath, P.K. Naicker, J. Chem. Eng. Data 48 (2003) 904–907.
[40] S.P. Verevkin, J. Safarov, E. Bich, E. Hassel, A. Heintz, Fluid Phase Equilib. 236 (2005) 222–228.
[41] M. Bendová, Z. Wagner, J. Chem. Eng. Data 51 (2006) 2126–2131.
[42] J.M. Crosthwaite, M.J. Muldoon, S.N.V.K. Aki, E.J. Maggin, J.F. Brennecke, J. Phys. Chem. B 110 (2006) 9354–9361.
[43] A. Heintz, T.V. Vasiltsova, J. Safarov, E. Bich, S.V. Verevkin, J. Chem. Eng. Data 51 (2006) 648–655.
[44] X. Hu, J. Yu, H. Liu, J. Chem. Eng. Data 51 (2006) 691–695.
[45] J. Safarov, S.P. Verevkin, E. Bich, A. Heintz, J. Chem. Eng. Data 51 (2006) 518–525.
[46] A. Shariati, C.J. Peters, J. Supercrit. Fluids 25 (2003) 109–111.
[47] L.P.N. Rebelo, J.N.C. Lopes, J.M.S.S. Esperança, E. Filipe, J. Phys. Chem. B 109 (2005) 6040–6043.
[48] J.O. Valderrama, P.A. Robles, Ind. Eng. Chem. Res. 46 (2007) 1338–1344.
[49] A. Klamt, J. Phys. Chem. 99 (1995) 2224–2235.
[50] A. Klamt, F. Eckert, Fluid Phase Equilib. 172 (2000) 43–72.
[51] A. Klamt, COSMO-RS from Quantum Chemistry to Fluid Phase Thermodynamics and Drug Design, Elsevier, Amsterdam, 2005.
[52] K.N. Marsh, A.V. Deev, C.-T. Wu, E. Tran, A. Klamt, Korean J. Chem. Eng. 19 (2002) 357–362.
[53] C.-T. Wu, K.N. Marsh, A.V. Deev, J.A. Boxal, J. Chem. Eng. Data 48 (2003) 486–491.
[54] U. Domańska, A. Pobudkowska, F. Eckert, J. Chem. Thermodyn. 38 (2006) 685–695.
[55] U. Domańska, A. Pobudkowska, F. Eckert, Green Chem. 8 (2006) 268–276.
[56] K. Sahandzhieva, D. Tuma, S. Breyer, A.P.-S. Kamps, G. Maurer, J. Chem. Eng. Data 51 (2006) 1516–1525.
[57] M.G. Freire, L.M.N.B.F. Santos, I.M. Marrucho, J.A.P. Coutinho, Fluid Phase Equilib. 255 (2007) 167–178.
[58] F. Eckert, A. Klamt, COSMOtherm. Version C2.1 Release 01. 05, COSMOlogic GmbH & Co. Kg, Leverkusen, Germany, 2005.
[59] F. Eckert, COSMOtherm User's Manual Version C2.1, Release 01.05, COSMOlogic GmbH & Co. Kg, Leverkusen, Germany, 2005.
[60] F. Eckert, A. Klamt, AIChE J. 48 (2002) 369–385.
[61] R. Ahlrichs, M. Bär, M. Häser, H. Horn, C. Kölmel, Chem. Phys. Lett. 162 (1989) 165–169.
[62] A. Schäfer, A. Klamt, D. Sattel, J.C.W. Lohrenz, F. Eckert, Phys. Chem. Chem. Phys. 2 (2000) 2187–2193.
[63] A. Schäfer, C. Huber, R. Ahlrichs, J. Chem. Phys. 100 (1994) 5829–5835.